Applied Thermal Engineering 149 (2019) 1454–1462

Contents lists available at ScienceDirect

Applied Thermal Engineering

journal homepage: www.elsevier.com/locate/apthermeng

Research Paper

Dynamic and steady state performance model of fire tube boilers with different turn boxes

Wim Beyne[a,b], Steven Lecompte[a,b], Bernd Ameel[a,b], Dieter Daenens[a], Marnix Van Belleghem[c], Michel De Paepe[a,b,*]

[a] Department of Flow, Heat and Combustion Mechanics, Ghent University, Sint-Pietersnieuwstraat 41, B-9000 Ghent, Belgium
[b] Flanders Make, The Strategic Research Centre for the Manufacturing Industry, Campus Arenberg Celestijnenlaan 300 – bus 4027, B-3001 Heverlee, Belgium
[c] Deconinck-Wanson, Legen Heirweg 43, 9890 Gavere, Belgium

HIGHLIGHTS

- A fire tube boiler heat transfer model is developed and validated.
- The effect of the turn box on overall performance is checked.
- Part load capability is investigated for several designs.
- Model variants are compared for accuracy and grid convergence.

ARTICLE INFO

Keywords:
Fire tube boiler
Turn box
Numerical model
Peak load capability

ABSTRACT

The market for fire tube boilers is increasingly demanding custom designs from the manufacturers. For these new designs, a comprehensive thermal model is needed. In this article, both a steady state and dynamic thermal model is developed based on the plug flow furnace model with general experimental correlations. The steady state model allows optimizing (i.e. safely downsizing) boiler designs. This model has been verified with measurement reports. The dynamic model is used to estimate the peak load capability of a boiler. In the presented case, the fire tube boiler can produce up to 2.5 times the nominal steam flow rate for a period of 10 min. Special attention has been paid to the turn boxes and their specific placement, which other models in literature neglect. The efficiency penalty of a non-submerged turn box can reach up to 12% but can be reduced significantly by insulation. Turn boxes also affect peak load capability. If the total length of the boiler is constant, submerging the turn box has a positive effect on the peak load capability. This effect is mostly attributed to the increased water volume. Finally, the article includes a comparison between the plug flow furnace model the ε-NTU method and the ε-NTU method with inclusion of radiation to model the tube passes. The ε-NTU method with inclusion of radiation allows to significantly reduce the necessary number of control volumes without reduction in the model accuracy.

1. Introduction

Fire tube boilers provide steam for a wide range of applications in the process industry. They operate at pressures up to 20 bar with steam flow rates up to tens of ton per hour. Compared to water tube boilers which produce steam up to 250 bar with flow rates in the range of hundred ton per hour, these are relatively low pressures and steam flow rates [1]. Consequently, water tube boilers are used for power production while fire tube boilers are mostly used for providing heat to industrial processes or municipal heat networks, combined heat and power grids and as peak boiler in larger grids.

Fig. 1 shows a schematic drawing of a fire tube boiler. The boiler consists of a large vessel, partially filled with water. The vessel contains a system of flue gas channels. The flue gas channels are heated by a burner and are submerged under water. If not submerged, the tubing could overheat leading to boiler failure [2,3]. By firing the burner, hot flue gasses are routed through the boiler and the water evaporates. Steam collects at the top of the vessel. The flue gas system consists of several heat exchangers. Firstly, there is the furnace in which the combustion takes place. The flue gas is then turned by a turn box and

* Corresponding author.
E-mail addresses: wim.beyne@ugent.be (W. Beyne), Michel.DePaepe@ugent.be (M. De Paepe).

https://doi.org/10.1016/j.applthermaleng.2018.09.103
Received 1 June 2018; Received in revised form 20 September 2018; Accepted 24 September 2018
Available online 25 September 2018

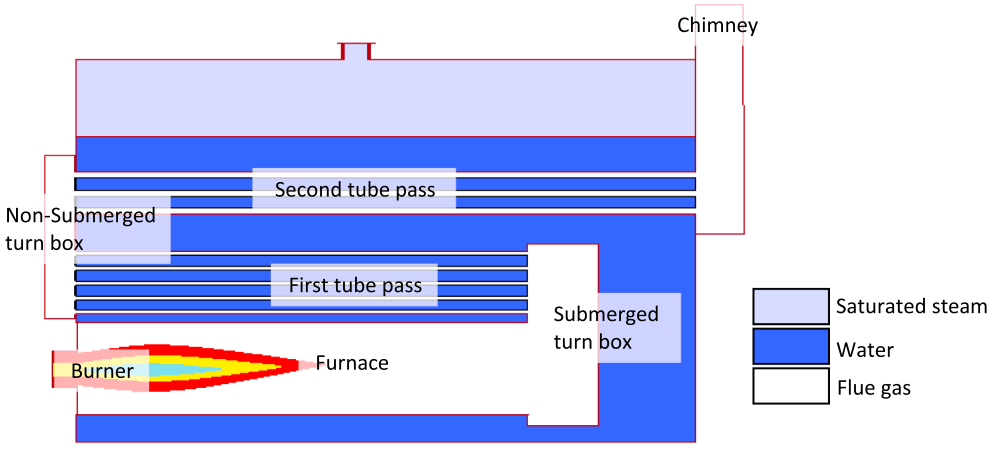

Fig. 1. Schematic drawing of a three pass fire tube boiler design with submerged turn box after the first pass and a non-submerged turn box after the second pass.

rerouted through the first tube pass. The furnace and the tube passes are called the gas passes. Turn boxes are thus the connection between the different flue gas passes. Gas flow in consecutive passes is reversed and therefore the primary goal of the turn boxes is to reverse the flow. There are two types of turn boxes: submerged and non-submerged. A submerged turn box acts as an extra flue gas pass, transferring heat to the water/steam mixture. In contrast, a non-submerged turn box causes a heat loss to the ambient. Additional heat losses that are incurred can be reduced by providing effective insulation. Fire tube boilers' construction can differ on two major aspects. Firstly, the number of flue gas passes can differ from typically a three pass boiler (e.g. furnace and two tube passes) to a four pass boiler. Depending on the number of tube passes, the flue gas is rerouted through the boiler two or three times (a three pass or four pass boiler). Secondly, there is the difference between a submerged and non-submerged turn box. Non-submerged turn boxes are cheaper to construct but result in a low thermal efficiency of the boiler.

There are two approaches to the thermal design of fire tube boilers. A first method is using standard catalogue designs characterized by a nominal steam production and pressure. Another way is with a thermal design model which can be used to make custom designs tailored to a client's need. A thermal design model can characterize a boiler both by steady state characteristics like the nominal steam production and by dynamic characteristics. These dynamic characteristics specify the ability of the boiler to deliver peak loads, one of the common operation modes of fire tube boilers.

A steady state model can serve as a design model [3–5]. These models all separate the fire tube boiler in three zones: a flue gas zone, a metal zone and the water/steam zone. All three models focus on the gas to metal heat transfer in the fire tubes. Although the shell side behavior is important in the operation of a fire tube boiler [6–8], it has a minor effect on the steady state heat transfer [5]. The major difference lies in the determination of heat transfer parameters. Huang et al. [5] experimentally fitted the well stirred furnace model [1] to a fire tube boiler while Rahmani et al. [2,4] divided the boiler in furnace and tube passes and estimated heat transfer coefficients using general correlations. Since the approach of Huang et al. [5] requires additional experiments, it cannot be used in the design stage. The approach by Rahmani et al. [3] can be used in the design phase but it does not include a description of the turn boxes. There is also no comparison between different modeling options for the tube passes. These modeling options are based on underlying assumptions on the importance of radiative heat transfer, and therefore a comparison can improve the understanding of heat transfer in the tube passes.

Several dynamic boiler models can be found in literature. Three of these models require limited or exhaustive experimentation [9–11]. For example Huang and Ko [9] expand the steady state model of Huang et al. [5] by adding the time derivatives to the conservation equations. The energy and mass content of the gas zone is neglected and the equations are linearized around an operating point. The model's parameters are determined by fitting the model to experimental data as a function of the firing rate and the steam operating pressure. This is in contrast to the steady state model, where the heat transfer was assumed to be constant over a large range of operating parameters. In contrast to Huang and Ko, Sørensen [12] does not use experiments to determine the heat transfer coefficients. However, experiments are used to determine the water level of the boiler. Where Huang and Ko [9] and Sørensen [12] use physical insight and a limited amount of experimentation, Vasquez et al. [10] use extensive experimentation to perform a systems identification of a fire tube boiler.

There are also models which do not require experiments [11,13,14]. Gutiérrez Ortiz [13] uses a similar model as Huang and Ko [9] but does not linearize the equations. The author presents both a rigorous model estimating the heat transfer and a simplified model. In the simplified model, the heat transfer is calculated as the product of the firing rate and an assumed efficiency, therefore it is not useful for evaluating the effect of design choices on heat transfer. The rigorous model was not implemented by Gutiérrez Ortiz and only a qualitative validation of the simplified model was made. Tognoli et al. [11] expanded the model presented by Gutiérrez Ortiz by applying the rigorous model. The resulting dynamic model is used to estimate variations in steam pressure due to a step in steam mass flow rate. The article highlights the possibility to significantly downsize boilers without loss of dynamic performance, however it does not investigate peak load performance. Bisetto et al. [14] developed a numerical dynamic model for a fire tube heat generator producing hot water. The three pass heat generator is divided into three zones: flue gas, metal and water volume. The flue gas and metal zone are subdivided in five control volumes: the furnace, two tube passes and two turn boxes. The effect of turbulators in the tube passes is investigated by CFD and experiments. The article however does not include a description of the peak load capabilities of the heat generator which is a major design criterion.

The present article first develops a steady state model for the heat transfer in the boiler which can be used for sizing novel boiler designs. In the tube passes, three model variants are compared: the plug flow model as used by Rahmani et al. [4] and, the effectiveness number of transfer units (NTU model) model with and without accounting for radiation. Furthermore, the steady state model investigates the effect of a submerged turn box on the efficiency of the fire tube boiler. It is verified using chimney temperature boiler data. Secondly, a dynamic model is developed which can determine the peak load capability. Peak loads are often encountered in boiler use and therefore should be estimated in the design phase. Besides the effect on efficiency, the effect of a submerged turn box on peak load capability is also examined.

Finally, the influence of the operational parameters on boiler peak load are investigated.

2. Steady state model development

The steady state model in this work is based on a three flue gas pass design with one submerged turn box, as shown in Fig. 1. An alternative design with the first turn box not submerged is also modeled and compared. The modelling approach is similar to the approach of Rahmani and Trabelsi [4], but includes the turn boxes. The steam boiler is considered as several heat exchangers in series, submerged in a uniform, saturated water volume. A two-phase water/steam zone, metal zone and gas zone are discerned. The model design comes down to determining the state of each zone and the heat transfer from one zone to another.

The two-phase water/steam zone is modelled by a single control volume and thermodynamic equilibrium between the phases is assumed. The evaporation pressure is imposed by the pressure set point of the control logic. The steam production is then equal to the ratio of the total heat transfer to the specific energy required to heat feed water to saturated steam.

The gas zones are divided into multiple control volumes for the furnace and tube passes and one control volume for each of the turn boxes. Expressing the conservation of mass, energy and momentum on the control volumes results in a set of equations which determines the gas and metal zone states. For a control volume i the conservation of energy in steady state is given by Eq. (1). In Eq. (1) the superscripts i and $i-1$ denote the control volume, $\dot{Q}_c$ denotes the combustion heat release and $\dot{Q}_{gm}$ denotes the heat transfer from flue gas to the metal.

$$\dot{m}_g(h_g^{i-1} - h_g^i) = \dot{Q}_c^i - \dot{Q}_{gm}^i \tag{1}$$

Since the heat transfer from gas to metal $\dot{Q}_{gm}$ is a function of the gas temperature, the left hand side of Eq. (1) is rewritten to solve for the gas temperature. This is done by rewriting the enthalpy difference as the product of the average specific heat capacity and the temperature. For the outlet enthalpy difference, this poses the issue that the specific heat capacity cannot be determined, as the outlet temperature is not known. In the work of Rahmani and Trabelsi [4] and Bisetto et al. [14], the specific heat capacity at the outlet temperature is assumed to be approximately equal to the specific heat capacity at the inlet of the control volume, resulting in Eq. (2).

$$T_g^i = \frac{1}{\dot{m}_g c_p^{i-1}}(\dot{Q}_c^i - \dot{Q}_{gm}^i) + T_g^{i-1} \tag{2}$$

However, this is only justified if the heat capacity difference over the extent of the control volume is negligible. This can be satisfied by increasing the number of control volumes, but at a penalty of increased calculation time.

An alternative to using Eq. (2) can be found by using an implicit scheme and solving the set of equations in an iterative manner. The gas enthalpy is linearized around the value found in a previous iteration. This results in Eq. (3), where the subscript 0 denotes the value obtained at the previous iteration.

$$h_g^i = h_{g,0}^i + c_{p,0}^i(T_g^i - T_{g,0}^i) \tag{3}$$

Substituting Eq. (3) in Eq. (1) results in Eq. (4).

$$T_g^i = T_{g,0}^i + \frac{1}{c_{p,0}^i}\left(\frac{1}{\dot{m}_g}(\dot{Q}_c^i - \dot{Q}_{gm}^i) + h_{g,0}^{i-1} + c_{p,0}^{i-1}(T_g^{i-1} - T_{g,0}^{i-1}) - h_{g,0}^i\right) \tag{4}$$

Using Eq. (4) to solve the temperature field in the furnace obtains a difference below 0.1% on the total heat transferred in the furnace for 100 control volumes compared to 200 control volumes. The difference remains below 1% with 20 control volumes while handling specific heat capacity differences of up to 9% between consecutive control volumes.

To solve the resulting set of equations, the heat transfer from one zone to another, the heat release by combustion and the pressure drop across the control volumes are determined.

2.1. Furnace and tube pass

The heat release by combustion is modelled by an exponential release law as is done by Gutiérrez Ortiz [13]. Rahmani and Trabelsi use a parabolic release law [4]. The release law should be fitted to the burner installed in the fire tube boiler. The heat transfer rate $\dot{Q}_{gm}$ between the gas and metal zone is modelled by the plug flow furnace model as shown in Eq. (5).

$$\dot{Q}_{gm} = g_{rad}\sigma(T_g^4 - T_{mi}^4) + h_c A_{mi}(T_g - T_{mi}) \tag{5}$$

g_{rad} denotes the total radiative heat transfer coefficient. Under the assumption of an infinitely long tube without axial radiation it can be written as Eq. (6) [1].

$$g_{rad} = A_{mi}\left(\frac{1-\varepsilon_m}{\varepsilon_m} + \frac{1}{\varepsilon_g}\right)^{-1} \tag{6}$$

A_{mi} is the inner metal surface area, ε_m the metal emissivity and ε_g the gas emissivity. The gas emissivity is determined using a polynomial approach by Taylor and Forster [15]. The correlation is valid between 1200 and 2400 K and takes both the gas temperature, the geometry of the enclosure and the partial pressure of CO_2 and H_2O into account. Outside this range, a correlation by Talmor is used [16] taking only the combustion gas composition into account. The emissivity correlations have large uncertainties up to 35% [17]. However the uncertainty on the emissivity and determination of g_{rad} resulted in an uncertainty on the total heat transfer of less than 0.2%.

The inner metal wall temperature T_{mi} is determined by an equivalent thermal resistance network, as used by Huang et al. [10]. The thermal resistance on the water side is determined using the nucleate boiling correlation of Cornwell [18] given by Eq. (7). In Eq. (7), d_o is the outside diameter, q the heat flux, λ the latent heat of evaporation, and μ the dynamic viscosity.

$$Nu = 100\left(\frac{d_o q}{\lambda \mu}\right)^{0.67} \tag{7}$$

In the tube bundles, a correction by Gorenflo [3] is made for the effect of closely packed tubes given by Eq. (8).

$$h = h_{st}\left(1 + \frac{1}{2 + q/1000}\right) \tag{8}$$

h_c denotes the convective heat transfer coefficient and is determined by the Gnielinski correlation [8]. The correlation determines a turbulent Nusselt number in the turbulent region ($Re > 4000$), a laminar Reynolds number in the laminar region ($Re < 2300$) and a linear interpolation based on the Reynolds number in the transition region. The turbulent correlation is given by Eq. (9).

$$Nu_{turb} = \frac{(\xi/8)(Re - 1000)Pr}{1 + 12.7\sqrt{\xi/8}\left(Pr^{\frac{2}{3}} - 1\right)}\left[1 + \left(\frac{d}{L}\right)^{2/3}\right]\left(\frac{T_b}{T_w}\right)^{0.45} \tag{9}$$

In Eq. (3), d is the tube diameter, L the tube length, T_b the bulk gas temperature, T_w the wall temperature and Pr the gas Prandtl number. ξ represents the friction factor for turbulent flow in tubes. It is determined by Eq. (10).

$$\xi = (1.8log_{10}Re - 1.5) \tag{10}$$

In the laminar regime, there is a difference between a uniform wall temperature and a uniform heat flux boundary condition. The wall temperature is closer to the water temperature than to the gas temperature as a result of the high heat transfer coefficient on the water side [4,5]. Since the water state is constant and uniform in the present

steady state model, the metal wall temperature will vary slightly along the flow length compared to the gas temperature. On the other hand, the varying gas temperature has a direct impact on the heat flux. Therefore, the uniform wall temperature boundary condition is adopted and Eq. (11) is used to determine the laminar Nusselt number. The effect of the thermal and hydraulic development length is taken into account.

$$Nu_{lam} = \left\{3.66^3 + [1.615\sqrt[3]{RePrd/L}]^3 + \left(\frac{2}{1+22Pr}\right)^{1/6}\sqrt{\frac{RePr}{L}}\right\}^3 \quad (11)$$

Eq. (5) is comprised of a radiative and a convective part. Radiation is less important in the tube passes and is therefore often neglected [2]. If convection is dominant, convection dedicated methods such as the ε-NTU method [9] can be applied. If radiation is important but not dominant, radiative heat transfer can be included by linearizing the radiative heat transfer as a function of the temperature difference. A radiative heat transfer coefficient given by Eq. (12) is added to the convective heat transfer coefficient.

$$\alpha = \frac{\sigma g_{rad}(T_g^4 - T_m^4)}{(T_g - T_m)} \quad (12)$$

The ε-NTU method needs less control volumes compared to the plug flow furnace model to accurately predict heat transfer. In this work, three models are made and compared. One model uses the plug flow furnace model in the tube passes (further called the PF variant), the other model uses the ε-NTU method in the tube passes (further called the NTU variant), the other model uses the NTU method but linearizes the radiation (further called the NTURAD variant). The results for both models are compared in the results section.

2.2. Turn boxes

The turn boxes are analyzed using similar equations as for a tube pass, but with adapted geometrical parameters. The submerged turn box is modelled using Eq. (1). The total radiative heat transfer coefficient g_{rad} is determined by Eq. (6). The flow pattern inside the turn boxes complicate the definition of the convective heat transfer coefficient. Several convective heat transfer phenomena occur. Firstly, there is the jet impingement of the flue gas from the furnace on the back wall of the submerged turn box. Secondly, the flow turns along the wall and enters the consequent turn box. To the authors' knowledge, no dedicated correlations exist. However, jet impingement on the back plate is expected to be dominant over the convection induced by the turned flow.

Therefore, the convective heat transfer coefficient is determined from correlations of jet impingement [5]. The metal temperature and waterside heat transfer are treated the same as for the furnace and tube passes.

The non-submerged turn box results in radiation losses to the ambient. Since the heat transfer coefficient on the flue gas side is larger (jet impingement, forced convection and radiation) than on the ambient side (radiation and natural convection at lower temperatures), the thermal resistance on the gas side is neglected. The inner wall temperature of the non-submerged turn box is thus taken as the flue gas temperature. The loss is determined by solving Eqs. (13) and (14).

$$\dot{Q}_{loss} = A\sigma(T_o^4 - T_{amb}^4) + \frac{1}{R_{tot}}(T_g - T_{amb}) \quad (13)$$

$$T_o = T_g - \dot{Q}_{loss}R_{cond} \quad (14)$$

A is the outer surface area, σ the Stefan Boltzman coefficient, T_o the outer wall temperature and T_{amb} the ambient temperature, R_{tot} is the total conductive and convective heat transfer resistance from the inner wall to the ambient and R_{cond} is the conductive heat transfer resistance of the turn box wall.

2.3. Pressure drop

Besides the temperature, the pressure drop is estimated. The momentum balance is solved, which accounts for the pressure changes due to the changing density. Frictional effects are taken into account by using the friction factor as determined by Filonenko [19] in the tube passes and the furnace, and a sharp elbow loss and entrance loss [20] for the turn boxes. The resulting system of equations is coupled with the energy conservation equations. However, a sensitivity analysis based on the model of Rahmani and Dahia [3] showed pressure losses have no significant influence on the temperature profile of the fire tube boiler. The momentum and energy equations can thus be solved separately. In the present article, the energy equation is first solved, afterwards the pressure equation is solved.

2.4. Verification

The model is verified using measurement reports on the operation of two boiler geometries. The measurements reports are taken as a required control on efficiency and performance of in situ boiler installation and were provided by Deconinck-Wanson in personal communication to the authors. The chimney temperature is measured at different burner firing rates, expressed as a firing rate. The firing rate is the power supplied by the burner expressed as a percentage of the nominal burner power.

For firing rates between 100% and 40% the maximum difference of the chimney gas temperature is 12 K (see Fig. 2). This is within the reported accuracy for Rahmani and Trabelsi's model [4]. At lower firing rates, both models are less accurate with a maximum error of 15 K for the PF model and 20 K for the NTU model. At high firing rates the PF model and NTU model give very similar results. This effect is further investigated in the results section of this paper.

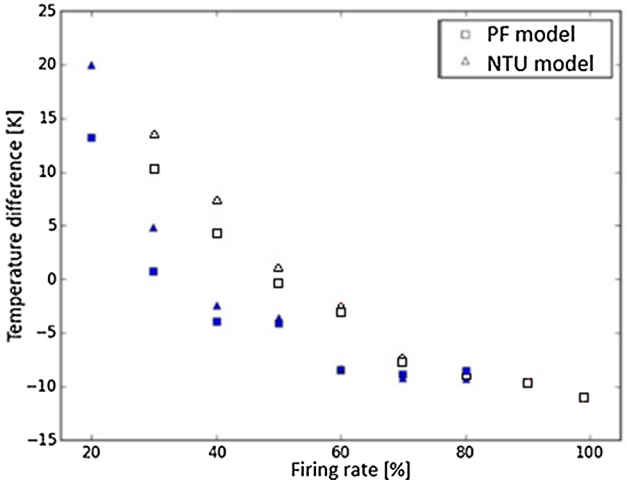

Fig. 2. Difference between calculated and measured chimney temperature; different color per measurement set.

The simulations in the remainder of the article are based on one of the boilers described in the measurement reports. The boiler characteristics are given in Table 1.

2.5. Model variants comparison

The model has to be implementable in a numerical optimization strategy to aid design. Numerical optimization typically requires a large amount of model calculations. Increasing the speed of the model is thus valuable. Therefore, an alternative model for calculating the heat transfer of the tube passes using an ε-NTU method [21] is investigated. The ε-NTU method allows describing heat transfer and temperature

Table 1
Boiler characteristics.

Power	1.252 MWth
Steam production	2 ton/h (~0.55 kg/s)
Steam content	947 l
Water content	4049 l
Length	3.75 m
Width	2.015 m
Height	2.42 m

distributions in convective dominated heat exchangers. The method solves the temperature distribution of the heat transferring fluids. However, several assumptions are necessary. Firstly, the fluid properties are assumed constant. Secondly, the radiation is either neglected or linearized with respect to the temperature difference. Using the ε-NTU allows reducing the number of control volumes compared to models which use an implicit Euler method. Since less control volumes are needed for the same accuracy, the model calculation time can be decreased. However, the ε-NTU method can only be applied if the temperature change is small enough for linearized radiation to hold. None of the models found in literature use the ε-NTU method, although Rahmani et al. [3] neglects radiation in the tube passes. In this paper, the applicability and advantages are assessed quantitatively for a specific case.

Three alternative models are compared: the plug flow model (PF), the ε-NTU model without radiation (NTU) and, the ε-NTU model with radiation (NTURAD). Their performance is analyzed both at nominal firing rate and at a reduced firing rate of 40%.

The thermal efficiency and chimney flue gas temperature are first used as performance criteria. The PF and NTURAD model calculate the same efficiency (up to 0.1%) and the same chimney temperature (up to 1 K) both at high and at low load. Yet the NTU model's results differ more strongly with a deviation of 0.5% in efficiency and 5 K in chimney temperature at low load. These are acceptable values with respect to the uncertainty of the model, therefore the global performance of the models is quite similar.

The local deviation of the gas temperature is a second, more local performance criterion. As for efficiency and chimney temperature, the PF and the NTURAD model results differ maximum 3.8 K with a root mean square deviation (RMSD) limited to 1.8 K. In contrast, the NTU model deviates up to 110 K which can be associated with neglecting of radiation in the tube passes by the NTU model. Remarkably, radiation makes up 25% of the heat transferred in the first and 12.5% of the heat transferred in the second tube pass. Furthermore, the NTU model's performance differs for high and low firing rates. The maximum temperature deviation and RMSD are higher at low loads than at high loads for the NTU model. This seems contradictory with the higher gas temperatures at high firing rate. However, the relative impact of the radiative fraction in the tube passes increases at low firing rates. As a result, the first tube pass heat transfer is underestimated by 8% by the NTU model when compared to the plug flow model. Due to increased gas temperature calculated at the start of the second tube pass, the heat transfer of the second tube pass is overestimated by 60% by the NTU model compared to the plug flow model. Therefore, models such as the model by Rahmani and Dahia [2] or the NTU model which neglect radiation in the tube passes are not capable of accurately estimating local gas parameters.

Although both NTURAD and PF model are suited for simulating fire tube boilers, they differ in terms of grid convergence. The convergence of heat transferred and chimney temperature is checked using the method of Roache [22] (Table 2). The error of the PF model for a grid of 5 control volumes is 18 K compared to 0.5 K for the NTURAD model. The NTURAD is thus superior to the PF model with respect to grid convergence and will be used in the remainder of this article. The used grid has 11 control volumes in the furnace and 5 control volumes in the tube passes, resulting in an error below 0.3 K for chimney temperature and 0.04% for total heat transferred. Note that all deviations of heat transfer rate are given normalized to the heat transfer calculated with the reference grid.

3. Dynamic model development

A dynamic model is developed to estimate the transient state of the boiler which includes the mass and energy content of the boiler. Similar to the steady state model, three zones are discerned: the flue gas, metal and water/steam zone.

3.1. Flue gas model

The state of the flue gas is of less significance for the boiler's performance than the metal and water/steam zone. Firstly, the energy content of the flue gas zone is two orders of magnitude smaller than the energy content of the other two zones. The driving force of the flue gas is larger than the driving forces for the metal and water zone. Therefore, the time constant of the flue gas zone's energy is orders of magnitude smaller than the other two zones. Secondly, the water/steam zone's mass content is orders of magnitude higher than the flue gas zone's mass content. Therefore, the time dependency of the flue gas zone's mass and energy content can be neglected. The resulting flue gas model is in steady state with the metal temperature. The steady state flue gas model can thus be reused in the dynamic model.

3.2. Metal zone model

The metal phase is divided into control volumes as is done in the steady state model. For each control volume, Eq. (15) expresses the conservation of energy. m denotes the metal's mass; c_m the metal's specific heat.

$$mc_m \frac{dT_m}{dt} = \dot{Q}_{gm} - \dot{Q}_{mw} \tag{15}$$

The heat transfer rate between metal and water/steam zone, $\dot{Q}_{mw}$, is calculated by assuming nucleate pool boiling. The Cornwell correlation is used to estimate the pool boiling heat transfer coefficient [18] with the Gorenflo correction in the tube passes [3].

The time derivative of the metal temperature $\frac{dT_m}{dt}$ is a function of the metal temperature T_m and the water temperature T_w. Since the water temperature varies slowly compared to the metal temperature, the metal zone is simulated assuming a constant water temperature. Sørensen [12] followed a similar approach for the development of a dynamic boiler model. As a result, the metal temperature as a function of time is determined by integrating Eq. (14).

Numerical integration can cause convergence problems with metal temperatures lower than the water temperature. To prevent these unphysical results, a smaller time step can be chosen. However, a smaller time step increases computational time. The problem can be avoided by rewriting Eq. (14) as an ordinary first order differential equation (ODE). Accordingly, the metal temperature at the next time step can be solved analytically. The analytical solution is inherently bounded by the water temperature and therefore it will not yield unphysical results.

Eq. (14) is rewritten as an ODE. Firstly, $\dot{Q}_{gm}$ and $\dot{Q}_{mw}$ are expressed as the products of a thermal conductance respectively S_g and S_w and the temperature difference between flue gas and metal, and metal and water. Substituting $\dot{Q}_{gm}$ and $\dot{Q}_{mw}$ in Eq. (15) results in Eq. (16). Afterwards, Eq. (16) is rewritten as an ODE given by Eq. (17). The coefficients a and b are defined by Eq. (17).

$$mc_m \frac{dT_m}{dt} = S_g(T_g - T_m) - S_w(T_m - T_w) \tag{16}$$

$$\frac{dT_m}{dt} = \frac{1}{mc_m}(S_g T_g - S_w T_w) - \frac{1}{mc_m}(S_g + S_w)T_m = a + bT_m \tag{17}$$

Table 2
Summarized result of grid convergence study of furnace, tube passes and total grid. The grid in the furnace and tube passes are compared to respectively 21 control volumes and 9 control volumes.

		Furnace grid			
Number of control volumes		6		11	
Deviation to the reference grid	Heat transferred in the furnace	0.3%		0.08%	
	Total heat transferred	0.01%		10^{-5}%	
	Chimney temperature	0.1 K		0.07 K	
		Tube passes grid			
		NTURAD	PF	NTURAD	PF
Number of control volumes		3		5	
Deviation to the reference grid	Heat transferred in the first tube pass	0.4%	4%	0.2%	3%
	Heat transferred in the second tube pass	2%	16%	0.8%	14%
	Total heat transferred	0.09%	0.7%	0.04%	0.5%
	Chimney temperature	1.25 K	33 K	0.5 K	18 K
		Total grid			
		NTURAD	PF	NTURAD	PF
Number of control volumes in furnace and tube passes		6–3		11–5	
Deviation to the reference grid	Total heat transferred	0.09%	0.7%	0.04%	0.5%
	Chimney temperature	1.2 K	24.7 K	0.3 K	9.7 K

Eq. (17) is solved which results in Eq. (18). The metal temperature at the next time step $T_m(t+\Delta t)$ can now be calculated if the metal temperature at the previous time step $T_m\ (t)$ is known.

$$T_m(\mathrm{t}+\Delta t) = \left(T_m(\mathrm{t}) + \frac{a}{b}\right)e^{\Delta t b} - \frac{a}{b} \tag{18}$$

3.3. Water/steam zone model

The water/steam zone's state is determined by both its mass and energy content. Only one control volume is used to simulate the water and steam mixture. As a result, the discrete-state space model is two dimensional: the total enthalpy and mass of the water.

Eq. (19) expresses the conservation of mass for the water/steam mixture. Three mass fluxes need to be determined. Firstly, the steam demand $\dot{m}_s$ is determined by the application. Therefore, it is an external input to the model. Secondly, the feed water $\dot{m}_{fw}$ is required to replenish the water in the boiler. The feed water keeps the water level in the boiler above a safety level to prevent tube burnout. The feed water supply system and control logic of the boiler fix the feed water mass flow rate. In the present study, an on-off control with a constant flow rate is applied. Thirdly, the boiler is periodically purged ($\dot{m}_p$) to decrease the concentration of impurities in the water. Since the concentration of impurities is not tracked, the purging water flow rate cannot be calculated by the model. Therefore, it is assumed to be a known boiler input.

$$\frac{dm_{ws}}{dt} = \dot{m}_{fw} - \dot{m}_s - \dot{m}_p \tag{19}$$

The conservation of energy of the water/steam mixture is expressed by Eq. (20). The total enthalpy is determined by integrating Eq. (20). The convective enthalpy flows and heat loss through the shell are integrated numerically. The total heat transfer from metal to water is integrated analytically as Eq. (21).

$$\frac{d(m_w h_w + m_s h_s)}{dt} = \sum \dot{Q}_{mw} + \dot{m}_{fw} h_{fw} - \dot{m}_s h_s - \dot{m}_p h_p - \dot{Q}_{loss} \tag{20}$$

$$\int_t^{t+\Delta t} \sum \dot{Q}_{mw}\, dt = S_w\left(\left(T_m(t) + \frac{a}{b}\right)\frac{1}{b}(e^{b\Delta t} - 1) - \Delta t\,(T_w + \frac{a}{b})\right) \tag{21}$$

The total state of the mixture is given by the total mass and the total enthalpy. Several terms on the right hand side of Eqs. (19) and (20) however depend on the thermodynamic state of the mixture. The feed water flow rate for example is determined based on the water level which depends on steam quality and temperature. The heat transfer from metal to water and from the steam/water mixture to the ambient are dependent on the water temperature as well. The thermodynamic state should thus be derivable from the total state.

The thermodynamic state of the two-phase mixture depends on the steam quality and any state variable. Two specific state variables can be determined. Firstly, the specific volume is calculated as the ratio of the fixed boiler volume to the mass of water and steam. Secondly, the specific enthalpy is the ratio of the total enthalpy of the mixture to the total mass. Both can be solved for the steam quality and the water/steam temperature.

4. Results

4.1. Effect of turn box position on boiler efficiency

The steady state model is used to estimate the boiler efficiency referenced to the fuel's lower heating value for a design with and without a submerged turn box. The boiler with submerged turn box is the design provided by Deconinck-Wanson, while the boiler with the non-submerged turn box has the same total length with a slightly elongated furnace and first tube pass and a smaller shell volume.

Fig. 3 shows the efficiency penalty incurred by using the non-submerged turn box both if the box is insulated with 5 cm of Rockwool and if it is not insulated. The efficiency decrease is about 8% for a non-insulated turn box and 1.1% for an insulated turn box at nominal load.

The loss of a non-submerged turn box can be strongly reduced by adding sufficient insulation. However, the chimney temperature of the boiler is higher for an insulated non-submerged turn box than for a non-insulated turn box. Efficiency assessments of boilers based solely on the chimney temperature without taking convective and radiative losses into account are therefore not useful to compare boilers.

The efficiency penalty decreases with increasing firing rate. The heat transfer resistance to the environment is dominated by the conduction through the walls and the natural convection at the outside of the turn box. Therefore, the heat transfer resistance is not significantly altered by an increased firing rate and cannot cause the decreased normalized losses. The temperature at the turn box however increase

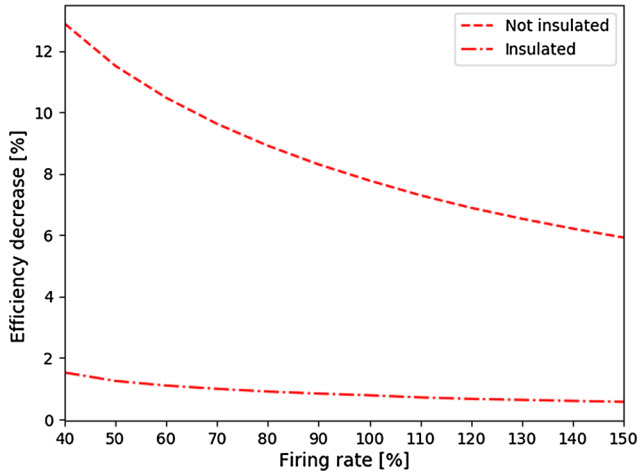

Fig. 3. Efficiency penalty for a non-submerged turn box compared to a submerged turn box for both insulated and non-insulated designs.

less than linearly with increased firing rate. Therefore, the normalized losses decrease with increasing firing rate.

Two major effects result in the efficiency penalty. Firstly, the non-submerged turn box results in a heat loss to the ambient. This loss is reduced by insulating the turn box. Since the efficiency penalty is reduced over fivefold by insulation, this first effect is dominant. Secondly, the submerged turn box is an extra heat exchanger in the fire tube boiler. The remaining loss due to this second effect is only 1.1% at nominal firing rate.

Taking only the second penalty effect into account, the efficiency loss of 1.1% should be about the contribution of a submerged turn box to the total heat transfer. However, when investigating the heat transfer contribution of heat exchangers in Fig. 4, the contribution of the turn box is about 6.8% referenced to the combustion heat. There are two alleviating effects explaining the lower efficiency loss. The first alleviating effect is the slightly increased size of the furnace and the first tube pass. The increased size does have a positive effect on the furnace heat transfer in Fig. 4, however the effect is insignificant. A second effect is the changed temperature at the start of the tube pass. In the case of an insulated, non-submerged turn box, the heat transfer rate is lower than for a submerged turn box. As a result, the temperature at the start of the first tube pass is increased which result in the higher tube pass contribution observed in Fig. 4. The increased heat transfer rate in

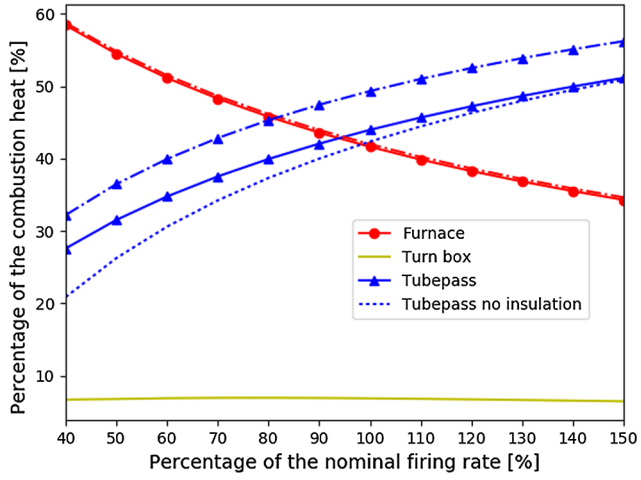

Fig. 4. Contribution of furnace (circles), turn box (full line) and tube pass (triangles) as a function of firing rate. The line style concerns three designs: full lines – submerged turn box, dash-dot lines – non-submerged insulated turn box, dotted lines – non-submerged and non-insulated turn box.

the tube passes diminishes the negative effect of losing a heat exchanger. The effect is detrimental for the not insulated turn box. In this case, the losses to the ambient are higher than the heat transfer to the water for a submerged turn box. The temperature and heat transfer rate is therefore lower in the tube passes.

For the three design variants, Fig. 4 shows clear trends in the contribution of each heat exchanger to the heat transfer. The furnace fraction decreases while the tube pass fraction increases and the turn box fraction remains quite constant. To understand the trend, the two major modes of heat transfer: convection and radiation are investigated. An increase in firing rate has two main effects. Firstly, an increased firing rate increases the average gas temperature which decreases the emissivity of the gas. Secondly with a higher firing rate, the gas mass flow rate is increased by a larger factor as the stoichiometric ratio of air to fuel is about 16 for the simulated natural gas. The increased mass flow rate has a positive effect on convective heat transfer. The increase is especially true for the first tube pass which transitions to laminar flow at lower firing rate. As a result of both effects, the ratio of heat transfer to firing rate increases for convection and decreases for radiation.

To understand the trends in Fig. 4, the contribution of radiation and convection in each heat exchanger is shown in Fig. 5 for a design with a submerged turn box. The furnace and first turn box are dominated by radiation while the tube passes are dominated by convection. As a result, the furnace fraction decreases with increasing firing rate. The decreased furnace fraction causes the temperature at the start of the turn box and the tube passes to increase. Since radiation dominates the submerged turn box, the turn box contribution remains quite steady. The tube pass is convection dominated, therefore the tube pass contribution increases with firing rate.

4.2. Estimating peak load capability

The peak load capability of a steam boiler depends on the control logic and set point of the boiler, the initial state of the boiler and the peak steam demand as a function of time. Therefore a method to characterize peak load capabilities must specify these three factors.

The control logic and set point determines the actions of the purging valve, burner and feedwater pump. The present method assumes prior knowledge of the steam peak demand. Therefore the burner is turned on from the start of the simulation to maximize the peak load capability. Furthermore the purging water flow rate is turned off. The feedwater control is on-off with a hysteresis between a high and low water level set point.

The steam demand is simplified to a step function between 0 and the steam peak which is a multiple of what is achievable in steady state. The steam peak value is expressed as a factor multiplied with the nominal steam flow rate. The peak is maintained until the boiler is no longer capable of delivering the steam at the minimum water pressure which is determined by the application. In the present case, the starting pressure is 8.5 bar the minimum pressure is 6 bar, the water level starts

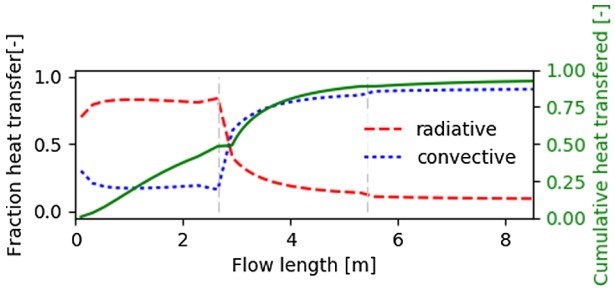

Fig. 5. Heat transfer along the flow length of the boiler. On the left axis: fraction of the heat transfer. On the right axis: the cumulative heat transferred (full line). Vertical dashed lines show the position of the two turn boxes.

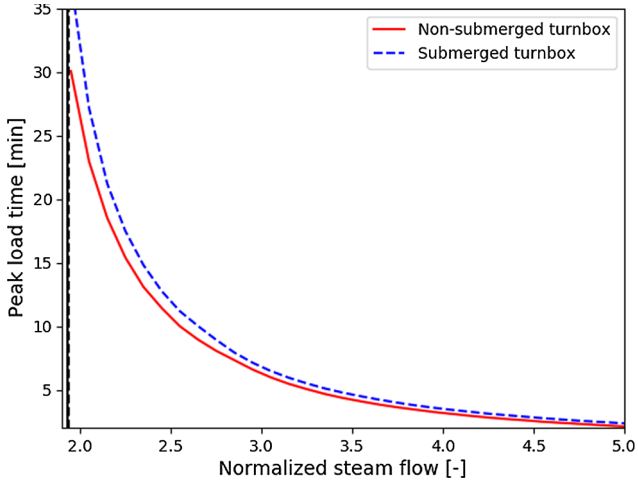

Fig. 6. Peak load capability for a boiler with a submerged and non-submerged turn box.

at 1.62 m with a minimum level of 1.37 m.

Fig. 6 shows the peak load times for both a boiler with a submerged and a non-submerged, insulated turn box. The black vertical lines indicate the steady state steam flow rate and define an asymptote to infinity for the peak load time. With increasing peak demand, the peak load time decreases to zero as more energy is extracted from the boiler. The boiler is capable of delivering steam demands in excess of 2,5 times the nominal steam load for a period of 10 min. This clearly shows the high potential of fire tube boilers for peak loads.

Unsurprisingly, the non-submerged turn box underperforms compared to the submerged turn box although the difference is limited. This is the result of both the lower efficiency and the lower shell volume of the boiler with a non-submerged turn box. To investigate the importance of both effects, a third boiler design with a non-submerged turn box but equal shell volume is simulated. The third boiler's peak load capability is quite similar to the first boiler's, therefore the dominant effect is the smaller water/steam volume for a non-submerged turn box design.

4.3. Effect of starting condition on peak load capability

In the previous section, the starting state of the boiler is fixed at a given pressure and a water level. However during operation, the pressure and water level in a boiler will oscillate between high and low levels determined by the control logic. Therefore, the starting state of the boiler can differ significantly between different situations. Furthermore, if there is prior knowledge available on a peak load, the starting condition can be controlled by adjusting firing rate and feed water flow rate. Clearly, firing the boiler will increase its energy content and therefore the peak load capability. Adding feed water however does not necessarily increase the peak load, since it can lead to a pressure drop.

The present section discusses the effect of starting pressure, water level and feed water flow rate. Figs. 7 and 8 show the result of a full factorial numerical experiment with ten levels of starting water height, pressure at a feed water mass flow rate. Both the water and pressure level are shown as a percentage between extreme operating conditions. The pressure level is varied between the maximum pressure level set in the control logic (9 bar) and the minimum pressure level set by the application (6 bar). These levels are clearly dependent on the boiler and application, therefore the peak load time plot will vary depending on the application. However, the trend is similar. The water level is varied between the minimum level of the boiler 1,37 m and the maximum level of the boiler 1,67 m. The steam peak is set at 5 times the value attainable in steady state while the feed water flow rate is set at 130%

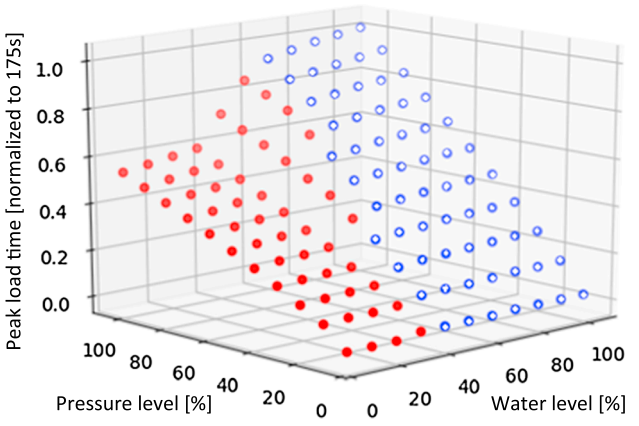

Fig. 7. Peak load time (normalized to 175 s) for a steam peak of 5 times the steady state value as a function of starting pressure (% scale between 6 and 9 bar) and water level height (% scale between 1,37 and 1,67 m). Filled circles are points with feed water flow, Empty circles do not have feed water flow rate.

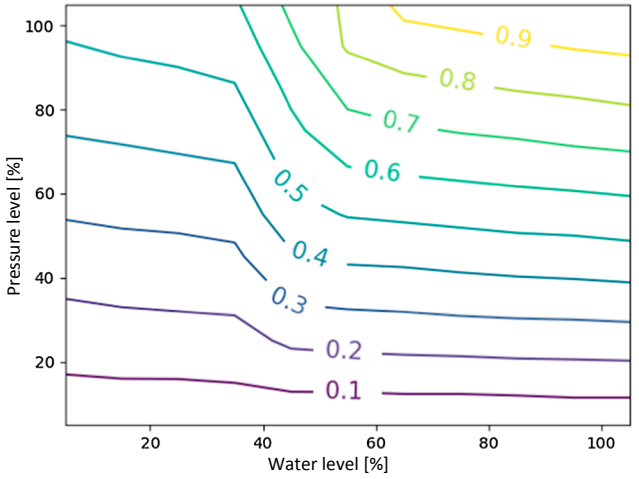

Fig. 8. Peak load time (normalized to 175 s) in a contour plot for a steam peak of 5 times the steady state value as a function of starting pressure (% scale between 6 and 9 bar) and water level height (% scale between 1,37 and 1,67 m).

of the steam peak.

Several operational zones can be distinguished on the plot. Firstly for both low and high water level, the pressure is dominant while the effect of increasing the water level is small. In between both zones, there is a transition area where the water level is important around 50% of the total scale. The transition area also marks the transition between the zone where the feedwater is used (filled circles) and the zone where it is not used (empty circles).

The boiler can fail because of either insufficient pressure level or insufficient water level. With a feedwater mass flow rate of 130% of the steam peak, all failures are due to insufficient pressure level. When the feedwater flow rate is reduced to 50% of the steam peak, the boiler fails due to insufficient water level for starting pressure higher than 7.5 bar and starting water levels below 10% of the total scale. In the case of a failure due to water level, increasing the feedwater flow rate has a positive effect on peak time. In the other case, increasing the feedwater flow rate has a negative effect on peak time with differences up to 65% for feedwater flow rates varying between 20% and 420% of the steam peak. The optimal feedwater flow rate in all cases is the lowest at which the boiler does not fail due to a low water level. The peak time of the boiler can thus be increased by adapting the feedwater flow rate to the steam peak as a function of starting pressure and water level.

5. Conclusion

Fire tube boilers are widely used in process industry. To optimize boiler design for a specific goal, a rigorous thermal model of a boiler is required. To the authors' knowledge, the present paper presents the most complete model currently available in literature and the only to include the thermal contribution of turn boxes.

A plug flow model, an effectiveness-NTU model including radiation and an effectiveness-NTU model without radiation for the tube passes were compared. Comparing the models showed that the model is not applicable at lower loads, due to the increasing importance of radiation at these loads. The NTURAD model including radiation obtained good results and was less sensitive to reducing the number of control volumes than the PF model.

Previously published models neglected the heat transfer in the turn boxes. However, submerged turn boxes contribute about 7% to the total heat transferred while non-submerged turn boxes can result in an efficiency penalty on the total efficiency as high as 12%. The penalty can be reduced by sufficient insulation and by elongating furnace and tube passes. Besides the effect on efficiency, turn boxes also influence the peak load capacity of the boiler. The peak load capacity is higher for the submerged turn box due to both an increased shell volume and an increased efficiency.

Finally, the sensitivity of peak load time to boiler initial state and feed water mass flow rate is investigated. Depending on the initial state, three zones are identified: zone without feed water flow, zone with feed water flow and a transition zone between. Adapting the feed water flow rate to the steam peak and the initial condition's zone allows increasing the peak time up to 65%.

Acknowledgements

Wim Beyne received funding from a Ph.D. fellowship strategic basic research of the Research Foundation - Flanders (FWO) (1S08317N). Steven Lecompte is a postdoctoral fellow of the Research Foundation-Flanders (FWO, 12T6818N). This research was supported by Flanders Make, the strategic research center for the manufacturing industry, Belgium.

Appendix A. Supplementary material

Supplementary data to this article can be found online at https://doi.org/10.1016/j.applthermaleng.2018.09.103.

References

[1] E.U. Schlunder, Heat Exchanger Design Handbook, Hemisphere Publishing, New York, NY, 1983.
[2] A. Rahmani, T. Bouchami, S. Bélaïd, A. Bousbia-Salah, M.H. Boulheouchat, Assessment of boiler tubes overheating mechanisms during a postulated loss of feedwater accident, Appl. Therm. Eng. 29 (2009) 501–508.
[3] A. Rahmani, A. Dahia, Thermal-hydraulic modeling of the steady-state operating conditions of a fire-tube boiler, Nucl. Technol. Rad. Protect. 24 (2009) 29–37.
[4] A. Rahmani, T. Soumia, Numerical investigation of heat transfer in 4-Pass fire-tube boiler, Am. J. Chem. Eng. 2 (2014) 65.
[5] B.J. Huang, R.H. Yen, W.S. Shyu, A steady-state thermal performance model of fire-tube shell boilers, J. Eng. Gas Turbines Power 110 (1988) 173–179.
[6] B. Maslovaric, V.D. Stevanovic, S. Milivojevic, Numerical simulation of two-dimensional kettle reboiler shell side thermal–hydraulics with swell level and liquid mass inventory prediction, Int. J. Heat Mass Transf. 75 (2014) 109–121.
[7] M. Pezo, V.D. Stevanovic, Z. Stevanovic, A two-dimensional model of the kettle reboiler shell side thermal-hydraulics, Int. J. Heat Mass Transf. 49 (2006) 1214–1224.
[8] G.V. Kuznetsov, S.A. Khaustov, A.S. Zavorin, K.V. Buvakov, V.A. Sheikin, P.A. Strizhak, et al., Computer simulation of the fire-tube boiler hydrodynamics, EPJ. Web Conf. 82 (2015) 01039.
[9] B.J. Huang, P.Y. Ko, A system dynamics model of fire-tube shell boiler, J. Dyn. Syst. Meas. Contr. 116 (1994) 745.
[10] J.R. Rodriguez Vasquez, R. Rivas Perez, J. Sotomayor Moriano, J.R. Peran Gonzalez, System identification of steam pressure in a fire-tube boiler, Comput. Chem. Eng. 32 (2008) 2839–2848.
[11] M. Tognoli, B. Najafi, F. Rinaldi, Dynamic modelling and optimal sizing of industrial fire-tube boilers for various demand profiles, Appl. Therm. Eng. 132 (2018) 341–351.
[12] K. Sørensen, Dynamic boiler performance – modelling simulating and optimizing boilers for dynamic operation, Aalborg Univ. (Denmark); Aalborg Industries A/S, Aalborg (Denmark), 2004.
[13] F.J. Gutiérrez Ortiz, Modeling of fire-tube boilers, Appl. Therm. Eng. 31 (2011) 3463–3478.
[14] A. Bisetto, D. Del Col, M. Schievano, Fire tube heat generators: experimental analysis and modeling, Appl. Therm. Eng. 78 (2015) 236–247.
[15] P.B. Taylor, P.J. Foster, The total emissivities of luminous and non-luminous flames, Int. J. Heat Mass Transf. 17 (1974) 1591–1605.
[16] E. Talmor, Combustion hot spot analysis for fired process heaters, Gulf Pub Co (1982).
[17] N. Lallemant, A. Sayre, R. Weber, Evaluation of emissivity correlations for H_2O-CO_2-N_2/air mixtures and coupling with solution methods of the radiative transfer equation, Prog. Energy Combust. Sci. 22 (1996) 543–574.
[18] B. Touhami, A. Abdelkader, T. Mohamed, Proposal for a correlation raising the impact of the external diameter of a horizontal tube during pool boiling, Int. J. Therm. Sci. 84 (2014) 293–299.
[19] V. Gnielinski, On heat transfer in tubes, Int. J. Heat Mass Transf. 63 (2013) 134–140.
[20] W.M. Rohsenow, J.P. Hartnett, Y.I. Cho, Handbook of Heat Transfer vol. 3, McGraw-Hill, New York, 1998.
[21] S. Kakac, H. Liu, A. Pramuanjaroenkij, Heat Exchangers: Selection, Rating, and Thermal Design, third ed., CRC Press, 2012.
[22] P.J. Roache, Quantification of uncertainty in computational fluid dynamics, Annu. Rev. Fluid Mech. 29 (1997) 123–160.

Michel De Paepe (1972) is professor of Thermodynamics in the Faculty of Engineering and Architecture at Ghent University. He graduated as Master of Science in Electro-Mechanical Engineering at Ghent University in 1995. In 1999 he obtained the PhD in Electro-Mechanical Engineering at Ghent University, graduating on 'Steam Injected Gas Turbines with Water Recovery'. In 2005 he spent 3 months as a visiting professor at the University of Pretoria (South Africa), doing research on flow regime detection.